# EVrich™ Exosome Automatic Isolation Instruments

JOT-EV02-02-01

## Product Overview

We independently developed here a magnetic bead-based high-throughput platform called EVrich™. It has been called EVrich™ for the isolation of EVs from urine while it is conceivable the system can be applied to other biofluids. The platform includes the EV capture, washing, and elution steps in the automated and paralleled mode.

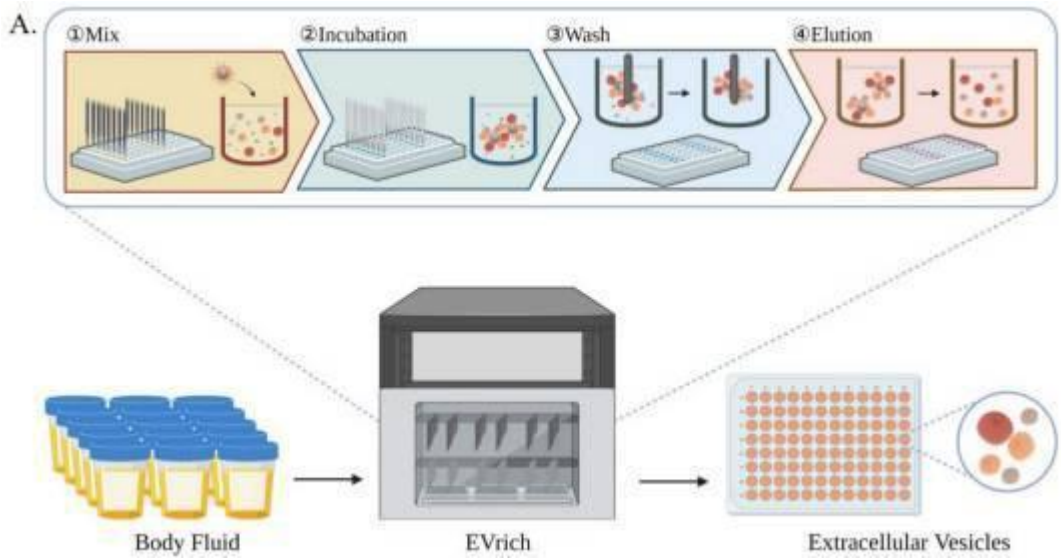


(A) A schematic overview of the automated EV isolation workflow, including the incubation, washing, and elution steps.

The platform provides an attractive and simple strategy for routine handling of clinical samples for EV studies, facilitating the translation of EV-based biology and research to clinical applications with minimal hands-on time and high throughput.

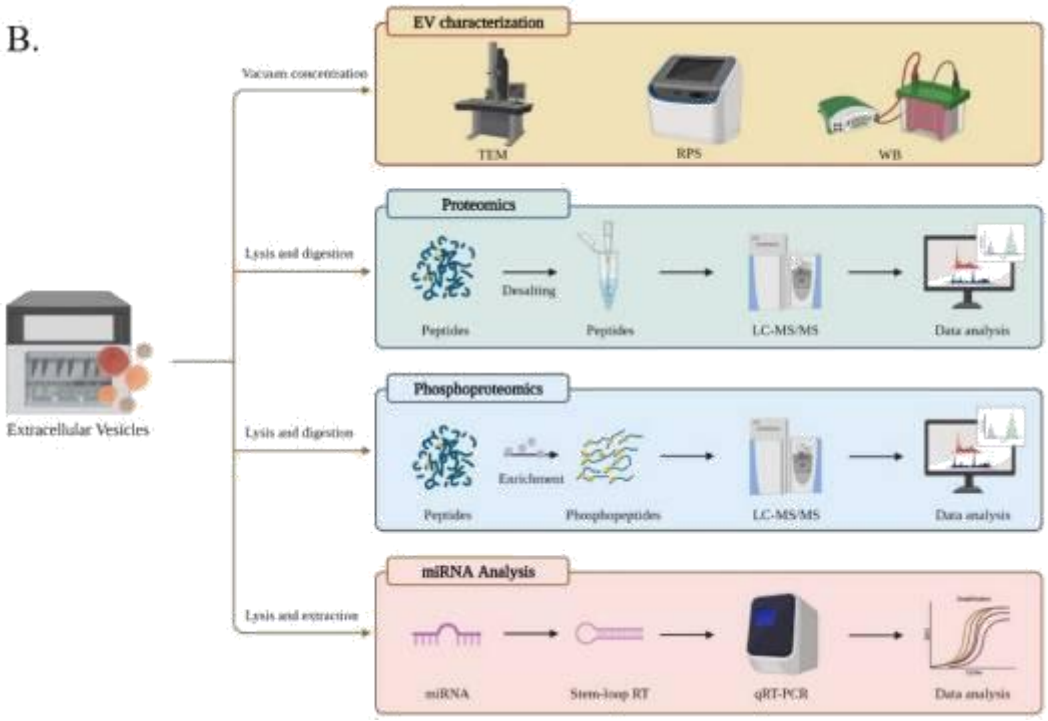


(B) The downstream EV analyses include EV characterization, EV proteomics, phosphoproteomics, and miRNA detection.

## Product advantages

To evaluate the performance of EVrich™ relative to the existing methods for EVs capture, we performed EV isolation and characterization by automated EVrich™, EVtrap™ manual, and UC. First, according to the TEM images (Figure 2A,B), the EVs isolated by the automated EVrich™ process demonstrated good size integrity, ranged in diameter from 50 to 150 nm, and showed a uniform spherical structure with a few impurities. Samples exhibited typical characteristics of extracellular vesicles. Figure 2C shows the RPS results of the three EV samples collected by manual EVtrap™, automated Evrich™, and UC. The result shows that EVrich might extract more small size (under 200 nm) EVs than manual or UC. Subsequently, the presence of the common EV marker TSG101, CD9, CD81, HSP70, and the absence of negative control Calnexin were validated by performing western blot analysis (Figure 2D). The band intensity from Evrich™ isolation was similar to that of the manual group but significantly higher than that of the UC group. The smaller intra -group variability of the

TSG101, CD9, CD81, and HSP70intensity in the automated group indicates the reliability and stability of the EVrich™ capture process. Calnexin is an endoplasmic reticulum protein, and Calnexin was not detected by the three methods, indicating that there was no protein contamination from cells in the extracted samples. In summary, the automated EV capture provides greater capture efficiency than UC while showing greater reproducibility and smaller variation than the manual operation.

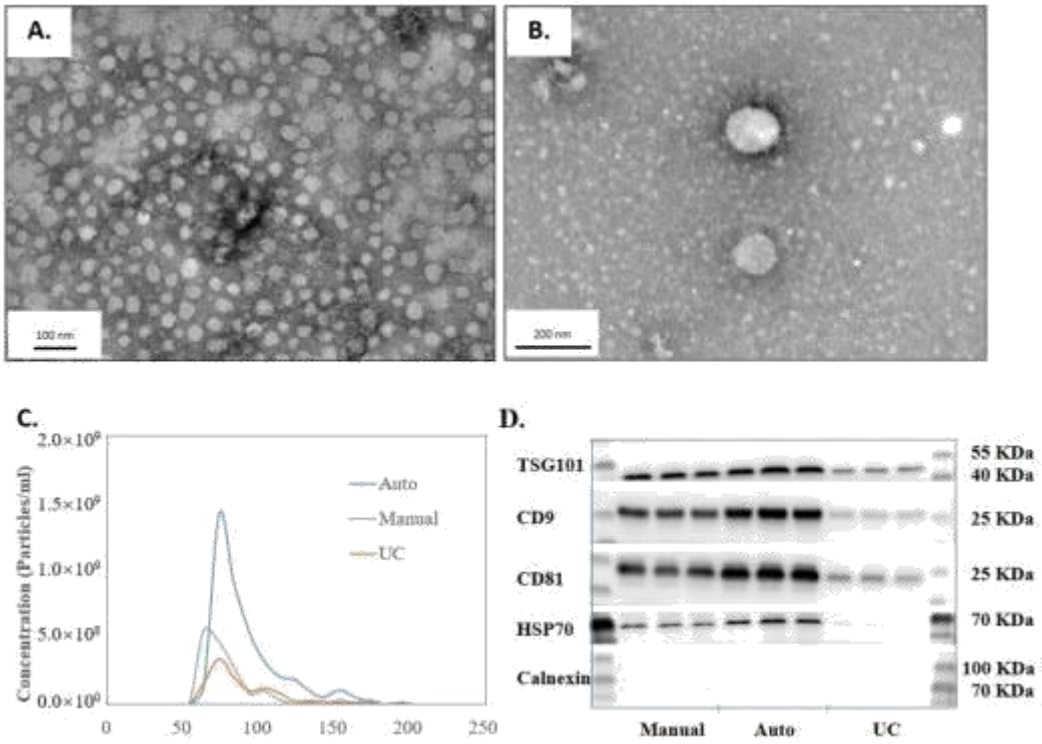


Figure 2

Characterization of the EVs isolated by EVrich™. (A,B) The transmission electron microscopy characterization of the EVs. (C) RPS (Range 60 nm–200 nm) characterization of EVs isolated by the three methods. (D) Western blot detection of the CD9 protein content isolated by the three methods.

To further demonstrate its application with clinical samples such as urine, we collected urine samples from three healthy donors twice a day for two consecutive days to confirm the stability of yield and purity when samples were loaded in different locations in the EVrich™ instrument (randomly selected) or processed on different days (Figure 3A). The WB results

(Figure 3B,C) show remarkably consistent CD9 signals on different days with three individuals.

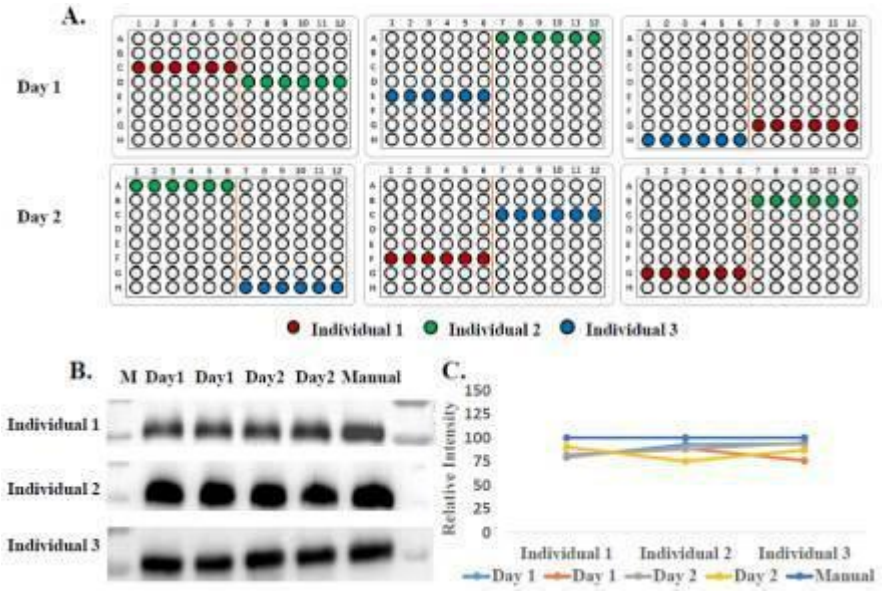


Figure 3

Stability assessment of the automated isolation. (A) The random sampling position sketch map of sample processing over two days. (B) Western blot analysis of CD9 signal from isolated EVs in urine. (C) Western blot CD9 quantitation from B.

The LC-MS/MS results showed that the signal intensities of the EV-specific proteins identified in manual and automated extractions were much higher than that after ultracentrifugation, while the signal intensities of representative contaminant proteins in urine were lower in manual and automated capture compared to UC (Figure 4A). Data obtained using the automated EVrich™ extraction were basically consistent with the manual EVtrap™ results. As shown in Figure 4B,C, we identified on average 14,600 unique peptides corresponding to ~2095 unique proteins in the manual capture group, which was quite similar to automated capture (on the average of 2074 proteins) and significantly higher than after ultracentrifugation (about 1390 proteins).

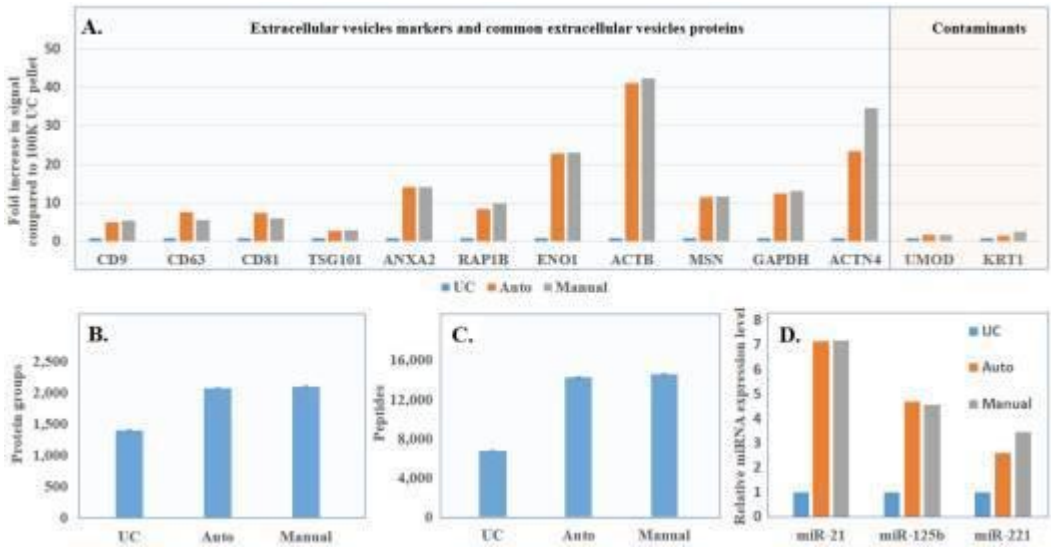


Figure 4
(A) LC-MS comparison of signal intensity of EV marker proteins and commons contaminants identified by the three isolation strategies. (B) LC-MS comparison of total EV proteins identified after isolation by the three different strategies. (C) LC-MS comparison of total EV peptides identified after isolation by the three different strategies. (D) Comparison of miRNA levels after isolation by the three different strategies.

Further, in-depth data analysis was employed to obtain statistical results and generate volcano plots and visualized heatmaps (Figure 5A–D). In comparison to prostatitis or prostatosis samples, the prostate cancer groups identified 268 overexpressed proteins and 186 overexpressed phosphorylated peptides corresponding to 48 phosphoproteins, which were illustrated in the volcano plots (Figure 5A,C).

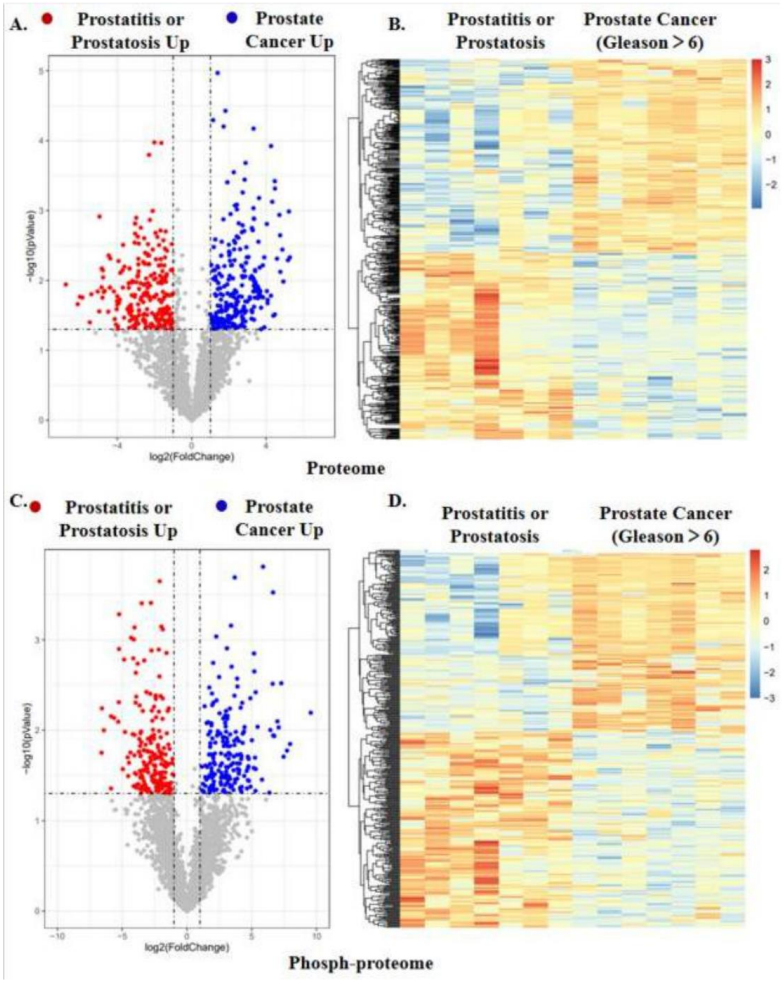


Figure 5

Results from quantitative proteomics and phosphoproteomics analyses of urine EVs from prostate cancer patients and prostatitis or prostatosis patients. (A) Volcano plot comparison of the regulated proteins. (B,C) Volcano plot comparison of the regulated phosphopeptides. (D) Heatmap of the significantly regulated overlapped phosphopeptides in the prostate cancer and control groups.